ADSORPTION MEASUREMENT OF CHLORINATED HYDROCARBONS INTO HIGH-SILICA ZEOLITE BY CHROMATOGRAPHIC METHOD

Kazuyuki Chihara, Kenta Saito, Hidenori Nakamura and Yosuke Kaneko
Department of Applied Chemistry, Meiji University
1-1-1 Higashi-mita, Tama-ku, Kawasaki Kanagawa 214 - 8571, Japan

Abstract

In this study, adsorption measurement of various chlorinated hydrocarbons on Y-type zeolites were performed using the chromatographic method to examine the adsorption phenomena. Dichloromethane (DCM), chloroform (TCM), trichloroethylene (TCE), and tetrachloroethylene (PCE), were used as the chlorinated hydrocarbons, and PQ-USY, USY-6.18, Na-Y, HSZ-390HUD, Pentasile-2 and Pentacil-1 were used as adsorbent. Each adsorption measurement was performed to get the heat of adsorption and the activation energy of micropore diffusivity. The amount adsorbed and isosteric heats of adsorption became low, when SiO_2/Al_2O_3 ratio of zeolite became high. The isosteric heats of adsorption were roughly 1.4 to 2.0 of the heats of vaporization. The activation energies of diffusion in the micropore of zeolite were found to be almost 40% to 60% of the isosteric heats of adsorption.

1. Introduction

Diffusion as well as adsorption equilibrium in adsorbent particles are important in designing adsorption processes. The possible mechanisms of diffusion in adsorbent particles are classified into three groups in the case of gaseous adsorption. They are diffusion in gas phase of macropores such as molecular diffusion or Knudsen diffusion, surface diffusion which occurs in the adsorbed phase, or diffusion in the micropores whose diameters are comparable with molecular diameter of adsorbates. The engineering estimation of the effective diffusivities for the first and second cases is almost possible, but when the intraparticle diffusion is controlled by the third mechanism, there are still some ambiguities in estimating the order of magnitude of the adsorption rate. Molecular sieving materials such as zeolite have micropores of well-defined structure. Micropores of zeolites have network structures. Study of micropore diffusion in molecular sieving materials is significant since they provide funda-mental characteristics of diffusion in other adsorbents which posses micropores of wide varieties. Though many investigations for intracrystalline diffusion in zeolite have been made, there has been, however, little work on diffusion of chlorinated hydrocarbons in zeolite.

Micropore diffusion of adsorbate molecules occurs in the potential energy field which is due to interactions between adsorbate molecules and adsorbent lattice atoms. This diffusion is generally described as each molecule hopping from one minimum of the potential energy distribution to another, or adsorption site to site, across potential energy barriers, which separate adjacent sites. This type of micropore diffusion is a kind of activated process and is called activated diffusion.

The purpose of this work is to experimentally determine the micropore diffusivities and adsorption equilibrium constants of various chlorinated organics in zeolite at wide temperature ranges and to correlate the obtained activation energies of micropore diffusion and isosteric heats of adsorption with the properties of adsorbate gases.

Chromatographic measurements were made for this purpose. By introducing the concentration pulse of adsorbate to the carrier gas stream at the inlet of the adsorbent column, the concentration elution curve at the outlet of the column was measured. Adsorption equilibrium constant and micropore diffusivity were determined by means of moment analysis of elution curves.

2. Experimental Procedure and Conditions

The experimental apparatus was shown in Figure 1. The apparatus was a conventional gas chromatograph (GC-9A) (Shimadzu Co., LTD). PQ-USY, USY-6.18, Na-Y, HSZ-390HUD, Pentasile-2 and Pentacil-1(crashed and screened to obtain particle size between #20 and #32) were used as adsorbent. These particles were packed in a column. The carrier gas was helium.

Dichloromethane, chloroform, trichloroethylene, and tetrachloroethylene were used as adsorbate. The adsorbate was introduced as pulse into the carrier gas stream by a 6-way valve. The flow was controlled by mass flow controllers (about 25 cm/sec). The outlet signal from the TCD cell was recorded to a chart-recorder and converted into personal computer as pulse response. Column conditions were shown in Table 1.

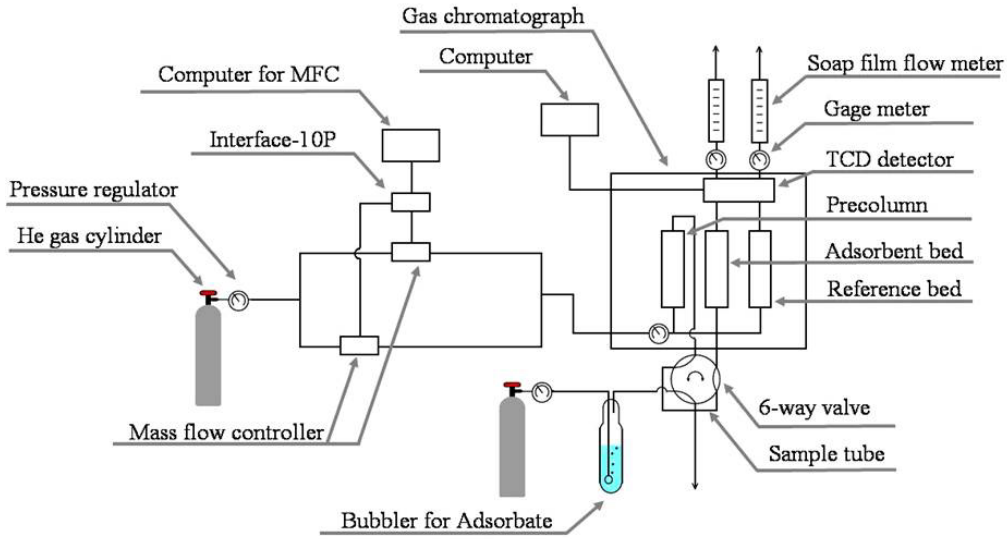

Figure 1 Experimental Apparatus

Table 1 column and adsorbent conditions

		HSZ-390HUD	PQ-USY	USY-6.18	Na-Y	Pentasile-1	Pentasile-2
Zeolite Type		FAU	FAU	FAU	FAU	MFI	MFI
SiO_2/Al_2O_3	[-]	460	70	6.18	5.6	400	30
Particle Density	[g/cm^3]	0.830	0.752	0.730	0.982	0.935	1.32
Macropore fraction	[-]	0.383	0.414	0.438	0.285	0.479	0.265
Bulk Density	[g/cm^3]	0.449	0.423	0.452	0.620	0.637	0.696
Void Fraction	[-]	0.460	0.428	0.385	0.369	0.319	0.473
Lenfth of Column	[cm]	47.21	30.0	30.1	25.0	24.0	18.5
Colmn Diameter	[cm]	0.30	0.30	0.30	0.30	0.30	0.30
Range of Sieve Openings	[mm]	0.495-0.833	0.495-0.833	0.495-0.833	0.495-0.833	0.495-0.833	0.495-0.833

3. Method of Analysis

The adsorption isotherm is given by a linear equation at near zero surface coverage:

$$q = K^* \cdot c \qquad (1)$$

where q= amount adsorbed per unit mass of adsorbent [g/g], K^*= adsorption equilibrium constant [cm^3/g], c= concentration in the fluid phase [g/cm^3].

The resultant moment equations of the impulse response for a packed bed of spherical particles with bidispersed pore structure and size distribution of the microparticles with helium carrier are (Chihara, Suzuki and Kawazoe 1978 and Kawazoe, Suzuki and Chihara 1973).

$$\mu_1 = \frac{z}{u}(1+\delta_0) \qquad (2)$$

$$\mu_2' = \frac{2z}{u}(\delta_d + \delta_f + \delta_a + \delta_i) \qquad (3)$$

where

$$\delta_0 = \frac{(1-\varepsilon)\varepsilon_a}{\varepsilon}\left(1+\frac{\rho_p K^*}{\varepsilon_a}\right) \qquad (4)$$

$$\delta_d = \frac{Ez}{u^2}(1+\delta_0)^2 \qquad (5)$$

$$\delta_f = \frac{1-\varepsilon}{\varepsilon}\cdot\frac{R}{3K_f}\left(\varepsilon_a + \rho_p K^*\right)^2 \qquad (6)$$

$$\delta_a = \frac{1-\varepsilon}{\varepsilon}\cdot\frac{R^2}{15D_a}\left(\varepsilon_a + \rho_p K^*\right)^2 \qquad (7)$$

$$\delta_i = \frac{1-\varepsilon}{\varepsilon}\cdot\frac{\rho_p K^*}{15D}\int_{-\infty}^{\infty} a^2 f(a)\, d\ln a \qquad (8)$$

The size distribution of the microparticles is assumed to be the log-normal distribution as

$$f(a) = \frac{1}{\sqrt{2\pi}\cdot\sigma}\exp\left[-\frac{(\ln a - \ln a_0)^2}{2\sigma^2}\right] \qquad (9)$$

By introducing Equation (9) into Equation (8), we get

$$\delta_i = \frac{1-\varepsilon}{\varepsilon}\cdot\frac{\rho_p K^*}{15D}\overline{a^2}\exp(\sigma^2) \qquad (10)$$

δ_f is neglected for its small effects in the following analysis. For instance, by using Carberry's equation (Carberry 1960), k_f can be estimated for the experimental condition. Then, the value of δ_f is found to be one order of magnitude smaller than δ_d or δ_a.

4. Result and Discussion

4.1 Microparticle size distribution

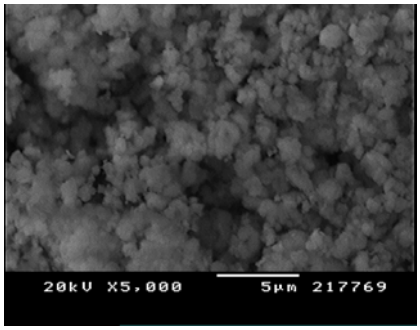

Figure 2 Photomicrograph of Pentasile-2 pellet

The size distribution of the microparticles for zeolite was determined by the scanning electron microscope. By cutting the zeolite pellet, the inner surface was photographed. A typical photomicrograph

is shown in Figure 2. It is apparent that the macroparticle is an agglomerate of microparticles, and the microparticles have random shapes and size distribution. The diameters in the same orientation of about 200 microparticles were measured from micrographs.

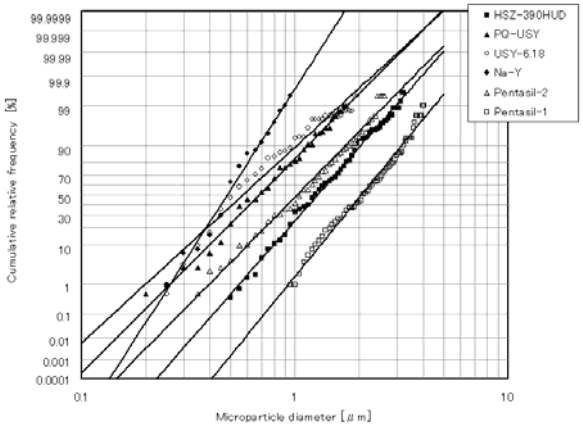

Figure 3 Log-normal size distribution of the microparticles of zeolite

On the assumption that the microparticle is a sphere, the cumulative number fraction was plotted against the microparticle radius $\bar{a}$ on a log-normal probability graph paper; straight lines were obtained as shown in Figure3. It is assumed that microparticles of zeolite have the log-normal size distribution. The radius at the peak of the probability a_0' which corresponds to a number fraction basis, and the standard deviation σ were thus found. In the case of log-normal distribution, the straight lines of distribution both on number fraction basis and on volume fraction basis are parallel on a log-normal probability paper, and the relation between the radius at the peak of the probability on a number fraction basis a_0' and that on a volume fraction basis a_0 and average radius $\bar{a}$ are as follows (Hatch 1933). The value of $\bar{a}$ and σ were shown in Table2.

$$a_0 = a_0' \exp\left(3\sigma^2\right) \tag{11}$$

$$\bar{a} = \frac{\int_{-\infty}^{\infty} af(a)d\ln a}{\int_{-\infty}^{\infty} f(a)d\ln a} = a_0 \exp\left(\frac{\sigma^2}{2}\right) \tag{12}$$

Table 2 Average radius and standard deviation

		HSZ-390HUD	PQ-USY	USY-6.18	Na-Y	Pentasile-1	Pentasile-2
Average Radius	[μm]	2.03	1.23	1.17	0.61	3.07	1.84
Standard Deviation	[-]	0.365	0.415	0.454	0.266	0.340	0.410

4.2 Moment analysis

The concentration of adsorbate in the effluent from the adsorbent bed was detected by the thermal conductivity cell. Figure 4 shows the effluent chromatographic peaks for dichloromethane pulses at several temperatures for almost the same velocity.

The first absolute moment and the second central moment were evaluated from the effluent peak $C_e(t)$ as follows:

$$\mu_1 = \int_0^{\infty} C_e(t)tdt \Big/ \int_0^{\infty} C_e(t)dt \tag{13}$$

$$\mu_2' = \int_0^{\infty} C_e(t)(t-\mu_1)^2 dt \Big/ \int_0^{\infty} C_e(t)dt \tag{14}$$

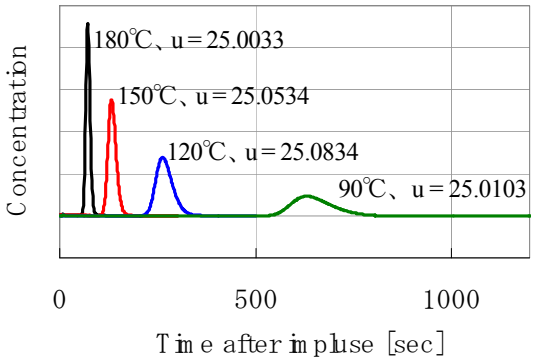

Figure 4 Typical chromatographic peaks for chloroform [HSZ-390HUD]

The analysis of second moment was simplified by first dividing Equation(3) by $[\mu_1/(z/u)]^2$ obtained from Equation(2). The result was

$$H = \frac{\mu_2'}{\mu_1^2}\left(\frac{z}{2u}\right) = H_0 + \frac{Ez}{u^2} \qquad (15)$$

where

$$H_0 = \frac{\delta_a + \delta_i}{(1+\delta_0)^2} \qquad (16)$$

Ez was expected to be proportional to u in the experimental condition. H_0 was able to be obtained as an intercept to the ordinate when H were plotted against $1/u$ according to Equation(15). Since δ_a could be estimated by the established evaluation equation for macropore diffusion and Equation(7), δ_i was obtained by Equation(16).

4.3 Adsorption equilibrium constant

Equation(2) and (4) were used along with the μ_1 to obtain the adsorption constant K^*. The isosteric heat of adsorption q_{st} is related with K^* for each gas by Van't Hoff's equation:

$$\frac{K^*}{T} = \left(\frac{K^*}{T}\right)_{\frac{1}{T}\to 0} \exp\left(\frac{qst}{R_g T}\right) \qquad (17)$$

Here it is assumed that the gas is ideal.

According to Equation(17), the obtained K^* divided by T was plotted against $1/T$ for various gases in Figure5, and the isosteric heat of adsorption q_{st} and $(K^*/T)_{1/T=0}$ were determined and listed in Table3.

Table 3 Properties of gases for adsorption

		HSZ-390HUD	PQ-USY	USY-6.18	Na-Y	Pentasil-1	Pentasil-2
DCM	ΔH[kJ/mol]			28.0			
	q_{st}[kJ/mol]	38.49	38.6	42.2	43.4	59.7	56.3
	E[kJ/mol]	13.39	19.3	23.3	13.7	33.4	43.4
TCM	ΔH[kJ/mol]			29.4			
	q_{st}[kJ/mol]	38.05	35.1	45.2	46.0	57.2	34.4
	E[kJ/mol]	13.33	19.0	39.4	30.3	40.5	8.7
TCE	ΔH[kJ/mol]			31.4			
	q_{st}[kJ/mol]	42.04	43.4	49.2	48.2	62.5	61.1
	E[kJ/mol]	11.22	17.9	20.1	10.8	39.0	30.0
PCE	ΔH[kJ/mol]			34.7			
	q_{st}[kJ/mol]	48.79	47.5	50.5	56.5	52.0	61.5
	E[kJ/mol]	17.87	12.8	21.3	40.1	34.6	38.5

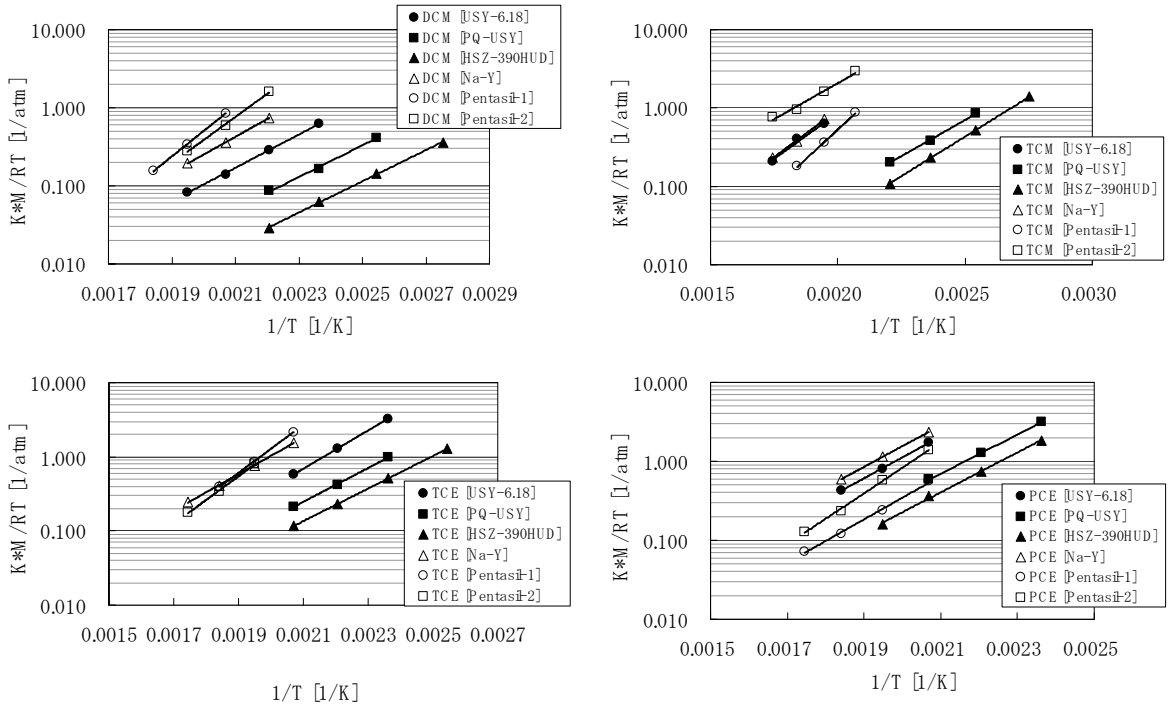

Figure 5 Van't Hoff plot of adsorption equilibrium

4.4 Axial dispersion

Equation(15) shows that the contribution of axial dispersion to H must be evaluated first to estimate H_0 from experimental value of H. In packed beds, Ez is expressed as a sum of a molecular diffusion(D_M) term and a term due to the velocity profile:

$$Ez = \frac{D_M}{\tau_{ext}} + \frac{d_p u}{Pe} \qquad (18)$$

The second term of equation(18) is expected to be dominant (Suzuki and Smith 1971), and H in Equation(15) should depend linearly on 1/u. Peclet number was evaluated(0.78) from the empirical correlation (Suzuki and Smith 1971) given as:

$$Pe=1.2dp \text{ :} dp \text{ in mm} \qquad (19)$$

4.5 Diffusion in macropore

H_0 includes the effect of the macropore diffusion and the micropore diffusion.
The following established relation (Satterfield 1970) was used to estimate the diffusivity in the macropore:

$$D_a = \frac{\varepsilon_a}{\tau_p} \cdot D_M \qquad (20)$$

where D_a= diffusivity in macropores D_M= molecular diffusivity ε_a =void fraction of macropore.
Equation (7) was then applied to estimate δ_a. Then, δ_i was obtained by Equation (16).

4.6 Diffusion in micropore

Since the size distribution of the microparticle for zeolite was already obtained by the electron microscope, diffusivities in micropores D were evaluated from δ_i and K^*, a, and σ by using Equation(10). The values of D for different temperatures were plotted according to the following Arrhenius' equation in Figure5.

$$D/\overline{a^2}\exp(\sigma^2)=\left[D_0/\overline{a^2}\exp(\sigma^2)\right]\exp\left(-\frac{E}{RT}\right) \qquad (21)$$

From Figure6, the activation energy E was determined from the slope of the straight line corresponding to the date points for each gas: the preexponential factor $D_0\exp(\sigma^2)$ was obtained as the interception to the ordinate at $1/T$=0. These figures were listed in Table3.

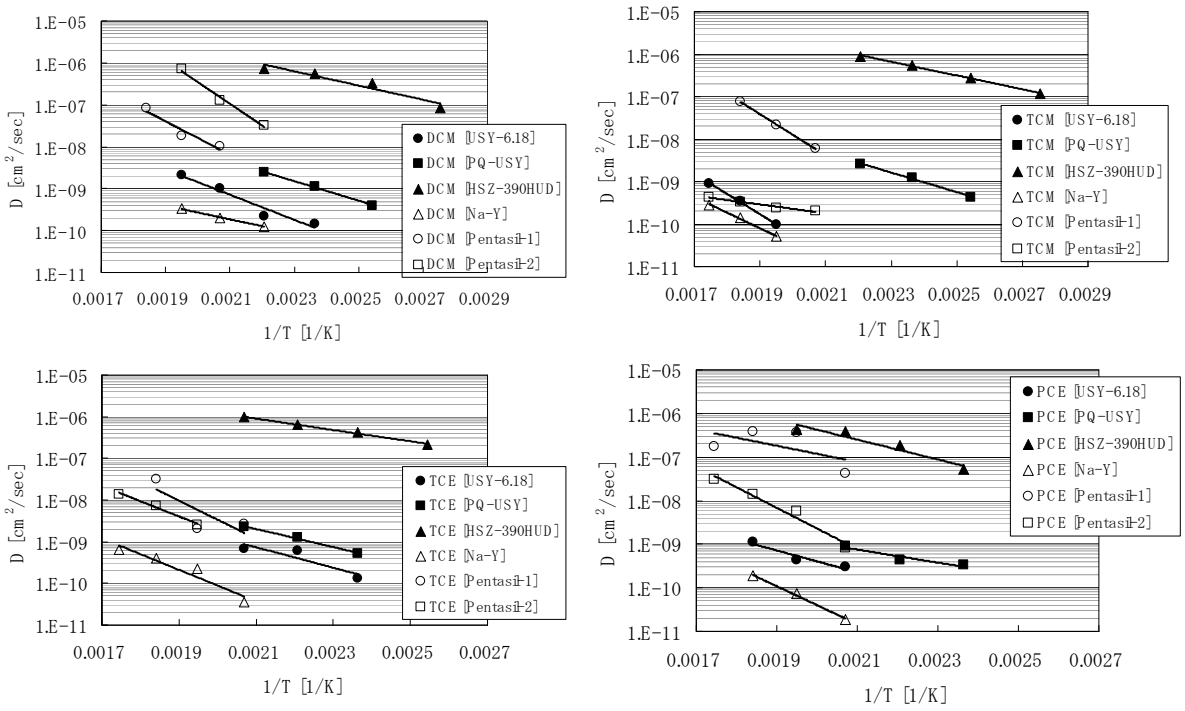

Figure 6 Arrhenius' plot

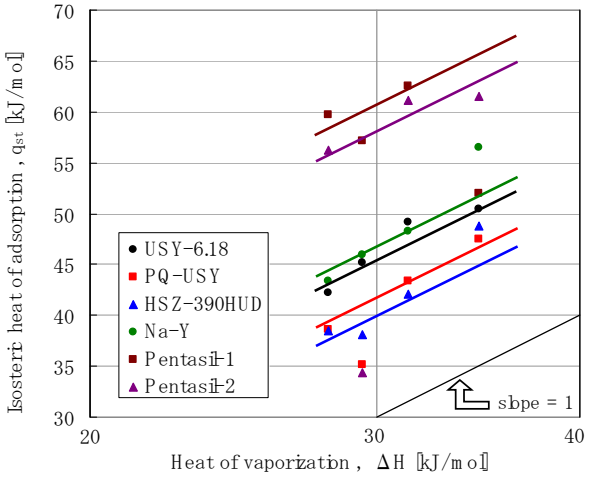

Figure7 Correction of isosteric heat of adsorption with heat of vaporization

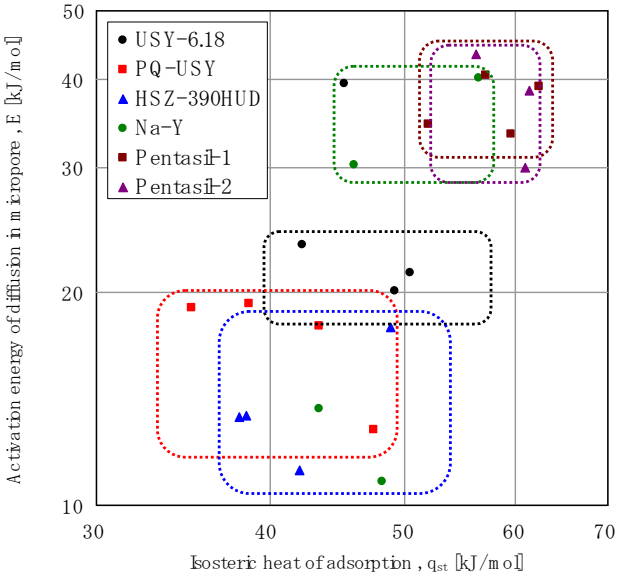

Figure8 Correlation of actibation energy of the micropore diffusion with isosteric heat of adsorption

4.7 Discussion

The isosteric heat of adsorption obtained with the chromatographic method of zeolite in this study is characterized, so that, the estimated values are for zero coverage, or initial isosteric heats of adsorption. Therefore, these values correspond entirely to the interaction between the adsorbate molecule and the adsorbent lattice atoms, excluding the interaction among adsorbate molecules.

Isosteric heat of adsorption q_{st} for five adsorbate with four adsorbent are plotted against the heat of vaporization ΔH of corresponding adsorbate in Figure 7. Here, The amount adsorbed and isosteric heats of adsorption became low, when SiO_2/Al_2O_3 ratio of zeolite became high. The isosteric heats of adsorption were roughly 1.4 to 2.0 of the heats of vaporization. (Barrer and Lee 1968) showed that the ratios $q_{st}/\Delta H$ for zeolite L slightly exceeded 2. Adsorption heat of PQ-USY is the lowest on all adsorbate. Adsorption heat of tetrachloroethylene became highest than others on all adsorbents.

Diffusion in the micropore of the zeolite is so called activated diffusion and is described as the molecules hopping from an adsorption site to another across the energy barrier which separates adjacent sites, which is similar to surface diffusion.

The activation energy was found to be half of isosteric heat of adsorption for the gases examined here.

5. Conclusion

Chromatographic measurements were made for various gas adsorptions on zeolite at three kind of temperatures, for zero coverage. Dichloromethane (DCM), chloroform (TCM), trichloroethylene (TCE), and tetrachloroethylene (PCE), were used as the chlorinated hydrocarbons, and PQ-USY, USY-6.18, Na-Y, HSZ-390HUD, Pentasile-2 and Pentacil-1 were used as adsorbent.

Adsorption equilibrium constants in the Henry's law region and diffusivities in the micropores in zeolite were determined from the first absolute moment and the second central moment where the effects of all the other possible transport processes in the case of bidispersed pore structure and also the log-normal size distribution of the microparticle were taken into account.

The amount adsorbed and isosteric heats of adsorption became low, when SiO_2/Al_2O_3 ratio of zeolite became high. The isosteric heats of adsorption were roughly 1.4 to 2.0 of the heats of vaporization. The activation energies of diffusion in the micropore of zeolite were found to be almost 40% of the isosteric heats of adsorption.

NOTATION

a = radius of microparticle, cm
a_0 = a at the peak of the probability on a volume fraction basis , cm
a_0' = a at the peak of the probability on a number fraction basis, cm
$\bar{a}$ = arithmetic average radius of microparticles defined
C_e = concentration in the effluent gas, mol/cm^3
c = concentration in the fluid phase, mol/cm^3
c = concentration in the particle, mol/cm^3
D = diffusivity in micropores based on amount adsorbed gradient driving force, cm^2/s
D_0 = preexponential factor for the Arrhenius' plot of D, cm^2/s
D_a = diffusivity in macropores, cm^2/s
D_M = molecular diffusivity, cm^2/s
d_p = particle diameter, cm
E = activation energy for micropore diffusion, kJ/mol
E_z = axial dispersion coefficient based on void spaces in the bed, cm^2/s
$f(a)$ = distribution function of the radii of microparticles
H = defined by Equation (13), s
H_0 = defined by Equation (14), s
ΔH = heat of vaporization, kJ/mol
K^* = adsorption equilibrium constant, cm^3/g
k_f = external mass transfer coefficient, cm/s
P_e = Peclet number, $d_p u/E_z f$
q = amount adsorbed per unit mass of adsorbent, mol/g
q_s = isosteric heat of adsorption, kJ/mol
R = radius of particles, cm
R_g = gas constant, Kcal/mol・K
T = absolute temperature, K
t = time, s
u = interstitial velocity of fluid, cm/s
v = volumetric flow rate, cm^3/s
z = longitudinal position in the bed, cm

REFERENCES

Barrer, R. M., Lee, A., Surface Sci., 12 341 (1968)
Carberry, J. J., AIChE, 6, 460 (1960)
Chihara, K., Suzuki, M., Kawazoe, K., AIChE, 24, 237-245 (1978)
Hatch,T.; "Determination of "Average Particles Size" from the Screen-Analysis of Non-Uniform Particulate Substances," J. Franklin Inst., 27, 215 (1933)
Kawazoe, K., Suzuki, M., Chihara, K., SEISAN-KENKYU, Japan, 25, 558 (1973)
Satterfield, C.N., M.I.T Press, London, 33 (1970)
Suzuki, M., Smith,J.M.,Chem., Eng. 3, 256 (1972)